Physica Scripta

PAPER

Temperature dependence of the correlation displacement functions of atoms under pressure effects for Cu_xAg_{1-x} alloy in EXAFS theory

Ba Duc Nguyen[1,*], **Trinh Phi Hiep**[1] **and Nguyen Van Thu**[2]

[1] Faculty of Physics, Tan Trao University, Tuyen Quang, Viet Nam
[2] Hanoi Pedagogical University 2, Viet Nam
[*] Author to whom any correspondence should be addressed.

E-mail: ducnb@daihoctantrao.edu.vn, trinhphihieptq@gmail.com **and** nvthu@hpu2.edu.vn

RECEIVED
21 January 2021

REVISED
22 June 2021

ACCEPTED FOR PUBLICATION
5 July 2021

PUBLISHED
13 July 2021

Keywords: anharmonic effective potential, correlation function, mean square displacement, local force constants, Debye model

Abstract

Reported here are expressions temperature dependence under pressure effects for the mean square displacement, the mean square relative displacement, the correlation displacement function of atoms, and the ratio of the relationship between the quantities due to anharmonicity under pressure effects in extended x-ray absorption fine structure spectra. The expressions are determined using the anharmonic correlated Debye model and the anharmonic Debye model. Complicated calculations due to the many-particle effects and anharmonic properties are replaced by a calculation based on the effective anharmonic potential, including the interaction of absorbing and scattering atoms with their nearest-neighbour atoms. Based on the Debye–Waller factor, the difference between the mean square relative displacement and mean square displacement is analyzed, and their ratios are calculated. This work is applied to face-centered cubic crystals and their alloys. Numerical results for copper (Cu-Cu), silver (Ag-Ag) crystals and copper–silver alloys Cu_xAg_{1-x} agree with experimental values and other studies.

1. Introduction

Thermal vibrations and disorder in Extended x-ray Absorption Fine Structure (EXAFS) give rise to the Debye-Waller factor (DWF). The DWF is considered to correlated averages over the Mean Square Relative Displacement (MSRD) σ^2 for a pair of absorber and backscatter atoms, in comparison, neutron diffraction refers to the Mean Square Displacement (MSD) u^2 of a given atom. The functions σ^2 and u^2 are closely related, from them, the displacement–displacement correlation function C_R can be deduced to describe the correlation effects in the vibration of atoms. The DWF plays an essential role in determining crystal structures as well as thermal quantities in EXAFS spectra. Many studies have derived methods for calculating and analyzing dependence on temperature of σ^2 (Tranquada and Ingalls 1983, Stern *et al* 1991, Frenkel and Rehr 1993, Duc *et al* 2018), u^2 (Beni and Platzman 1976, Schowalter *et al* 2009), and the correlation effects between them for cubic crystals (Nguyen *et al* 2020). However, to date have not been studies the temperature dependence under pressure effects of σ^2, u^2 and atomic correlation displacement functions for intermetallic alloys.

In the present work, how the correlation displacement function depends on temperature and pressure is analyzed and described by the function $C_R(T, P)$ based on the DWF in EXAFS. Analytical expressions are determined for $\sigma^2(T, P)$ based on the anharmonic correlated Debye model (ACDM) and for $u^2(T, P)$ based on the anharmonic Debye model (ADM), and the ratio relationships among $\sigma^2(T, P)$, $u^2(T, P)$, and $C_R(T, P)$ are considered. The effects of multi-particle systems are accounted for in the present one-dimensional model by means of a simple measure based on the derived anharmonic effective potentials, including the interactions of absorber and backscatter atoms with their nearest neighbours. Single-pair interactions of atoms are described by the Morse potential. This study analyzes the difference between σ^2 obtained from the ACDM and u^2 from the ADM, applies the analytical expressions to face-centered cubic (fcc) crystals and intermetallic alloys, and presents numerical results for copper (Cu-Cu), silver (Ag-Ag) crystals and copper–silver alloys Cu_xAg_{1-x}. Here,

$Cu_{72}Ag_{28}$ is the alloy with 72% of Ag and 28% of Cu, and $Cu_{50}Ag_{50}$ is the alloy with 50% of Cu and 50% of Ag (or 1:1 ratio). Some authors have studied these materials previously (Nguyen and Vu 2019, Ba 2020), and the results obtained using the present theory agree well with experimental values (Greegor and Lytle 1979, Kraut and Stern 2000, Okube and Yoshiasa 2001, Pirög *et al* 2002) and other study (Beni and Platzman 1976, Ba and Tho 2017).

This study chooses Cu_xAg_{1-x} (x = 72, 50) inter-metallic alloys because (1) $Cu_{72}Ag_{28}$ (±1%) and is also known as CuSil or UNS P0772 (note: CuSil should not be confused with Cusil-ABA, which has the composition 63.0% Ag, 35.25% Cu, and 1.75% Ti). CuSil is a eutectic alloy usually used in engineering, and the material is mainly used to weld metal in a vacuum environment (Nafi *et al* 2013). (2) For $Cu_{50}Ag_{50}$, an alloy discovered by Kraut and Stern that does not exist at the 1:1 ratio experimentally in 2000, so far there has been no theory to explain and confirm, especially the non-existent alloy over the entire temperature range or at only a given temperature range. Therefore, these issues need to be considered and studied.

2. Formalism

In the anharmonic approximation, EXAFS spectra are usually expressed as (Frenkel and Rehr 1993)

$$\chi(\kappa) = \sum_j \frac{S_0^2 N_j}{\kappa \Re_j^2} F_j(\kappa) e^{-2\sigma_j^2\kappa^2} e^{-2\Re_j/\lambda} \sin[2\kappa\Re_j + \delta_j(\kappa)], \tag{1}$$

where S_0^2, N_j, $F(k)$, $\delta(k)$, $\Re_j$, κ, and λ are defined elsewhere (Crozier *et al* 1988, Frenkel and Rehr 1993). In equation (1), the exponential function $2\sigma_j^2\kappa^2$ is the Debye–Waller factor (DWF), and the coefficient σ_j^2 is the MSRD of the bond between two nearest-neighbor atoms (Hung and Rehr 1997). During neutron diffraction or x-ray absorption, the DWF has the similar form of $(1/2)\kappa^2 u_j^2$.

In the atoms' vibration, convention r is the distance between two atoms at temperature T and is represented by the difference

$$r_j = \hat{\Re}_j^0(\boldsymbol{v}_j - \boldsymbol{v}_0), \tag{2}$$

Here, $\hat{\Re}_j^0$ is the unit vector for atom j at equilibrium, $\boldsymbol{v}_j$ is the displacement vector of atom j, and $\boldsymbol{v_0}$ is the displacement vector of the absorber atom located at the coordinate origin.

In equation (1), the MSRD σ^2 is defined while taking the exponential average $\langle \exp(2i\kappa r_j)\rangle$ (Crozier *et al* 1988)

$$\langle \exp(2i\kappa r_j)\rangle \rightarrow \langle \exp[2i\kappa\hat{\Re}_j^0(\boldsymbol{v}_j - \boldsymbol{v}_0)]\rangle = \exp(-2\kappa^2\langle[\hat{\Re}_j^0(\boldsymbol{v}_j - \boldsymbol{v}_0)]^2\rangle). \tag{3}$$

For the harmonic-approximation oscillation, the expression for the MSRD σ^2 dependence on temperature and under pressure effects has the form

$$\sigma_j^2(T, P) = \langle[\hat{\Re}_j.(\boldsymbol{v}_j - \boldsymbol{v}_0)]^2\rangle = \langle(\boldsymbol{v}_j.\hat{\Re}_j)^2\rangle + \langle(\boldsymbol{v}_0.\hat{\Re}_j)^2\rangle - 2\langle(\boldsymbol{v}_0.\hat{\Re}_j)(\boldsymbol{v}_j.\hat{\Re}_j)\rangle. \tag{4}$$

With $\boldsymbol{v}_0 = \boldsymbol{v}_j$, the MSD $u^2(T, P)$ is expressed as

$$u_j^2(T, P) = \langle(\boldsymbol{v}_0.\hat{\Re}_j)^2\rangle = \langle(\boldsymbol{v}_j.\hat{\Re}_j)^2\rangle, \tag{5}$$

and the correlation function $C_R(T, P)$ is expressed as

$$C_R(T, P) = 2\langle(\boldsymbol{v}_0.\hat{\Re}_j)(\boldsymbol{v}_i.\hat{\Re}_j)\rangle. \tag{6}$$

From equations (4)–(6), the MSRD, MSD, and correlation function are related by

$$C_R(T, P) = 2u_j^2(T, P) - \sigma_j^2(T, P). \tag{7}$$

To determine the functions $\sigma^2(T, P)$, $u^2(T, P)$, and $C_R(T, P)$ with anharmonic effects, we must determine the effective spring force constants (SFCs) of atomic pairs in a cluster of nearest-neighbours atoms, and this is done based on the effective anharmonic potential as a function of the displacement x under pressure effects. According to the ACDM (indexed as A) and ADM (indexed as D), the anharmonic potential has the following form (Okube and Yoshiasa 2001, Hung *et al* 2014):

$$U_{eff}^{A/D}(x) \approx \frac{1}{2}k_{eff}^{A/D}x^2 + k_{3eff}^{A/D}x^3, \tag{8}$$

where $k_{eff}^{A/D}$ is the effective SFC, $k_{3eff}^{A/D}$ is the cubic parameters (CP) that causes the asymmetry of the interaction potential due to anharmonicity, $x = r - r_0$ is the lattice thermal expansion, and r is the distance between two atoms at temperature T and pressure P, and r_0 is the corresponding value at equilibrium and pressure 0GPa. The difference between the SFCs and CPs leads to the difference between the potentials $U_{eff}^A(x)$ and $U_{eff}^D(x)$ in equation (8).

The SFCs and CPs can be obtained when the effective potentials are determined under temperature and pressure effects with different magnitudes. We write M_1 for the mass of the absorbing atom and M_2 for that of the scattering atom, and mass of two atoms can be considered as of an atom with mass $\mu = M_1M_2/(M_1 + M_2)$ and located at the midpoint of the distance two atoms, μ is the reduced mass.

In the ACDM, the potential $U_{eff}^{A}(x, P)$ has the form

$$U_{eff}^{A}(x, P) = U(x, P) + \sum_{j\neq i} U\left(\frac{\mu}{M_i} xP\hat{\Re}_{12}.\hat{\Re}_{ij}\right), \tag{9}$$

where $U(x, P)$ is the interaction potential between the absorber and backscatter atoms. The sum of i over absorber ($i = 1$) and backscatter ($i = 2$) atoms and the sum of j over their nearest neighbours in a cluster of atoms describe the lattice contributions to pair interactions and depend on the crystal structure type. In equation (9), $\hat{\Re}$ is the unit vector. For fcc crystals, the potential $U_{eff}^{A}(x, P)$ is written as

$$U_{eff}^{A}(x, P) = U(x, P) + 2U\left(-\frac{x}{2}, P\right) + 8U\left(-\frac{x}{4}, P\right) + 8U\left(\frac{x}{4}, P\right). \tag{10}$$

Similarly, according to the ADM, the potential $U_{eff}^{D}(x, P)$ is the expression of the single-particle effective potential, and when only the influence of the N nearest-neighbour atoms is taken into account, the potential $U_{eff}^{D}(x, P)$ is

$$U_{eff}^{D}(x) = \sum_{j=1}^{N} U(xP\hat{\Re}^{\mathbf{0}}.\hat{\Re}_j). \tag{11}$$

For fcc crystals, we have

$$U_{eff}^{D}(x, P) = U(x, P) + U(-x, P) + 4U\left(\frac{x}{2}, P\right) + 4U\left(-\frac{x}{2}, P\right). \tag{12}$$

Using the effective potentials in equations (10)–(12) changes the complex three-dimensional problem for multi-particle effects into a more straightforward one-dimensional problem.

Expanding the Morse potential $U(x, P)$ to third order around a minimum point gives

$$U(x, P) = Y(e^{-2\phi xP} - 2e^{-\phi xP}) \approx Y(-1 + \phi^2x^2P^2 - \phi^3x^3P^3 + ...), \tag{13}$$

where Y is the dissociation energy and $1/\phi$ corresponds to the width of the potential. It is usually sufficient to consider weak anharmonicity (i.e., first-order perturbation theory) so that only the cubic term in equation (13) must be kept. For two-component intermetallic alloys, if the two-component symbols of the alloy have the indexes 1 and 2, then we have ϕ_{12} and Y_{12}, and their values are calculated as a percentage doping of alloy (Duc and Tho 2019, Nguyen 2020).

According to the Debye model, the SFCs are expressed as

$$k_{eff}^{A/D} = aY_{12}\phi_{12}^2, \qquad k_{3eff}^{A/D} = -bY_{12}\phi_{12}^3. \tag{14}$$

For the ACDM, the factors are $a = 5$ and $b = 3/4$, and for the ADM they are $a = 8$ and $b = -1$.

Having derived the thermodynamic quantities in equations (5)–(7), we describe the system in the Debye model with all the different frequencies, each corresponding to a wave of frequency $\omega(q)$, where the wavenumber q varies in the first Brillouin region. Based on the ACDM, the expression for $\sigma^2(T,P)$ has the form

$$\sigma^2(T, P) = \frac{\hbar c}{2\pi k_{eff}^{A}} \int_0^{\pi/c} \omega_A(q) \frac{1 + z_A(q)}{1 - z_A(q)} dq, . \tag{15}$$

$$z_A(q) = e^{-(\beta\hbar\omega(q))}, \qquad \omega_A(q) = 2\sqrt{\frac{2k_{eff}^{A}}{M}} |\sin(qc/2)|, \qquad \beta = \frac{1}{k_B T}. \tag{16}$$

Upon substituting k_{eff}^{A} from equation (14) into equations (15) and (16), $\sigma^2(T)$ has the form

$$\sigma^2(T, P) = \frac{\hbar c}{10\pi Y_{12}\phi_{12}^2} \int_0^{\pi/c} \omega_A(q) \frac{1 + z_A(q)}{1 - z_A(q)} dq, \tag{17}$$

$$z(q) = e^{-(\beta\hbar\omega_A(q))}, \qquad \omega_A(q) = 2\sqrt{\frac{10Y_{12}\phi_{12}^2}{M}} |\sin(qc/2)|, \qquad |q| \leqslant \pi/c. \tag{18}$$

Similarly, for the ADM, $u^2(T)$ is determined as

$$u^2(T, P) = \frac{\hbar c}{2\pi k_{eff}^{D}} \int_0^{\pi/c} \omega_D(q) \frac{1 + z_D(q)}{1 - z_D(q)} dq, \tag{19}$$

Table 1. Parameters Y_{12} and ϕ_{12} for Morse potential at pressure P = 0GPa.

Quantity/ Crystal	Y_{12} [eV] (Present)	Y_{12} [eV] (Expt.)	ϕ_{12} [Å^{-1}] (Present)	ϕ_{12} [Å^{-1}] (Expt.)
Cu-Cu	0.3429	0.3528	1.3588	1.4072
Ag-Ag	0.3323	0.3253	1.3690	1.3535
$Cu_{72}Ag_{28}$	0.3381	—	1.3634	—
$Cu_{50}Ag_{50}$	0.3376	—	1.3638	—

Table 2. Effective spring force constants and cubic parameters.

Quantity/ Crystal	k^A_{eff} [eV Å^{-2}] (Present)	k^A_{eff} [eV Å^{-2}] (exp.)	k^D_{eff} [eV Å^{-2}] (Present)	k^D_{eff} [eV Å^{-2}] (Exp.)	k^A_{3eff} [eV Å^{-3}] (Present)	k^A_{3eff} [eV Å^{-3}] (Exp.)	k^D_{3eff} [eV Å^{-3}] (Present)	k^D_{3eff} [eV Å^{-3}] (Exp.)
Cu-Cu	3.1655	3.4931	5.5889	5.7520	0.6646	0.8070	3.0889	2.9831
Ag-Ag	3.1139	2.9797	5.8547	5.9032	1.0753	1.2289	3.4674	3.0563
$Cu_{72}Ag_{28}$	3.1423	—	5.0278	—	0.6814	—	2.6874	—
$Cu_{50}Ag_{50}$	3.1396	—	5.0234	—	0.6423	—	0.8569	—

Table 3. Morse potential parameters, spring force constants and cubic parameters under pressure effects for $Cu_{50}Ag_{50}$.

Pressure[GPa]	Y_{12} (eV)	ϕ_{12} (Å^{-1})	k^A_{eff} (eVA^2)	k^D_{eff} (eVA^2)	k^A_{3eff} (eVA^3)	k^D_{3eff} (eVA^3)
0	0.3376	1.3588	3.1396	5.0234	0.6423	0.8569
5	0.3154	1.3485	2.9032	4.8756	0.6415	0.8426
10	0.2977	1.3168	2.7428	4.6843	0.5902	0.8215
14	0.2184	1.2854	2.3595	4.4782	0.5527	0.7927

$$z_D(q) = e^{-(\beta\hbar\omega_D(q))}, \qquad \omega_D(q) = 2\sqrt{\frac{2k^D_{eff}}{M}}\,|\sin(qc/2)|, \tag{20}$$

Substituting k^D_{eff} from equation (14) into equations (19) and (20) gives

$$u^2(T, P) = \frac{\hbar c}{16\pi Y_{12}\phi_{12}^2}\int_0^{\pi/c}\omega_D(q)\frac{1+z_D(q)}{1-z_D(q)}dq, \tag{21}$$

$$z_D(q) = e^{-(\beta\hbar\omega_D(q))}, \qquad \omega_D(q) = 2\sqrt{\frac{8Y_{12}\phi_{12}^2}{M}}\,|\sin(qc/2)|, \qquad |q| \leqslant \pi/c, \tag{22}$$

where c is the lattice constant, q is the phonon wavenumber, and M is the mass of composite atoms. From equations (7), (17), (18), (21), and (22), we have the correlation function $C_R(T,P)$ as

$$C_R(T, P) = \frac{\hbar c}{8\pi Y_{12}\phi_{12}^2}\int_0^{\pi/c}\omega_D(q)\frac{1+z_D(q)}{1-z_D(q)}dq - \frac{\hbar c}{10\pi Y_{12}\phi_{12}^2}\int_0^{\pi/c}\omega_A(q)\frac{1+z_A(q)}{1-z_A(q)}dq. \tag{23}$$

3. Numerical results and discussion

We use equations (17), (21), (23) to perform calculations for Cu-Cu, Ag-Ag and Cu_xAg_{1-x}. The results of the theoretical calculations of the parameters of the Morse potential at pressure 0GPa and the experimental Morse parameters (Okube and Yoshiasa 2001) are listed in table 1, and the SFCs are listed in table 2. The data in tables 1 and 2 show that the theoretical calculations agree with the experimental measurements and other studies (Greegor and Lytle 1979, Tranquada and Ingalls 1983, Yokoyama *et al* 1989, Okube and Yoshiasa 2001, Pirög *et al* 2002). Table 3 listed results of theoretical calculations for Morse potential parameters, spring force constants and cubic parameters with effects of pressure up to 14GPa for $Cu_{50}Ag_{50}$ alloy. Substituting the parameters in tables 1–3 into equations (17), (21), and (23) gives $\sigma^2(T, P)$, $u^2(T, P)$, and $C_R(T, P)$ for Cu–Cu, Ag–Ag and Cu_xAg_y.

There is a significant difference between the correlation oscillation model and the single-particle anharmonic oscillation model, and this difference is due to the determination of the number and mass of atoms

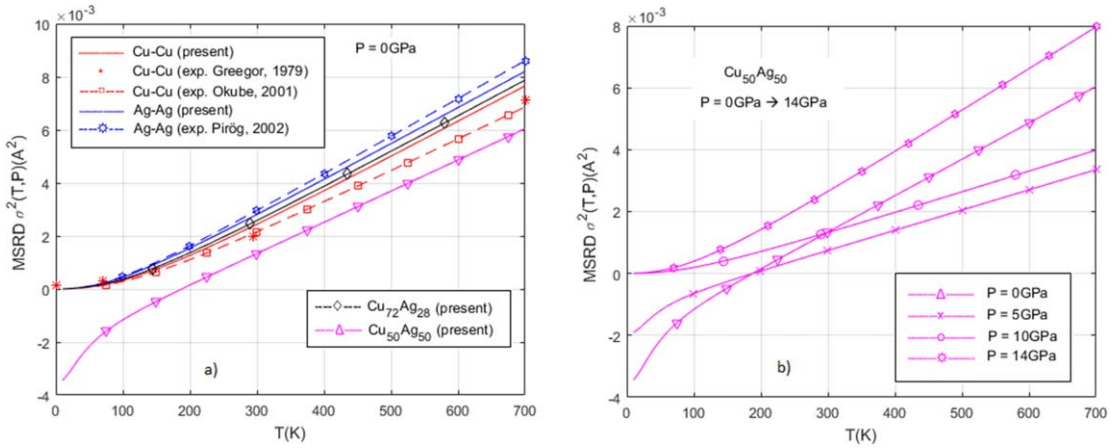

Figure 1. Dependence on temperature and pressure of σ^2(T, P) for Cu, Ag, Cu_xAg_{1-x} (x = 72, 50) at 0GPa (a); For Cu_xAg_{1-x} (x = 50) up to 14GPa (b).

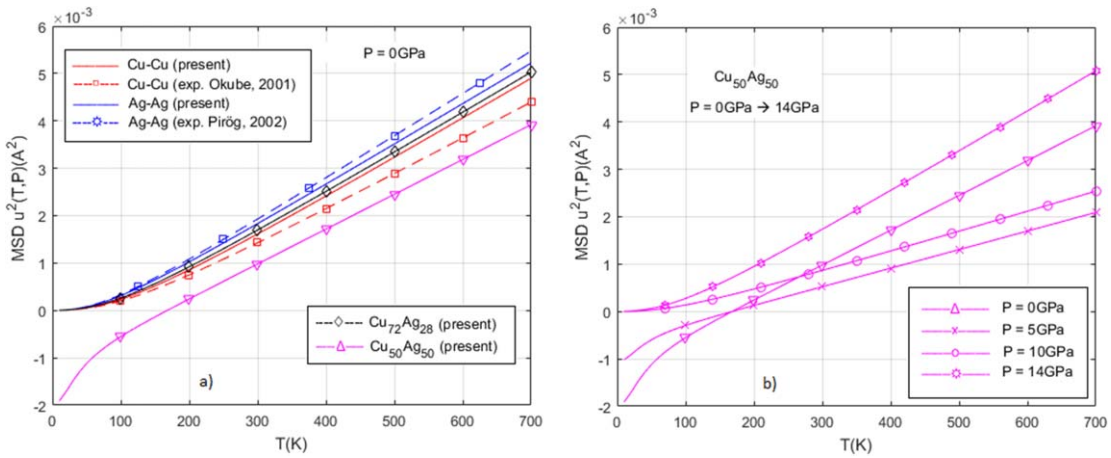

Figure 2. Dependence on temperature and pressure of u^2(T, P) for Cu, Ag, Cu_xAg_{1-x} (x = 72, 50) at 0GPa (a); For $Cu_{50}Ag_{50}$ up to 14GPa (b).

oscillating in the two models. For the correlation oscillation model, the particles' quantity and mass are only half of those of the single-particle anharmonic oscillator, and a crystal acts as quasi-atoms. That means that the mass is reduced to only half of the composite atomic mass, and the number of atoms is only half that for a single-particle anharmonic vibration model.

Figures 1 and 2 show the temperature dependences of σ^2 and u^2, respectively, for Cu-Cu, Ag-Ag, and Cu_xAg_{1-x} ($x = 72, 50$) at pressure 0GPa (figures 1(a), 2(a)), and pressure up to 14GPa (figures 1(b), 2(b)) for Cu_xAg_{1-x} (x = 50); $\sigma^2(T, P)$ and $u^2(T, P)$ are both linearly proportional to the temperature T at high temperatures, and $\sigma^2(T, P)$ is greater than $u^2(T, P)$ at any given temperature, and this is seen more clearly in figures 1(a), 2(a), the experimental values of $\sigma^2(T, P)$ for Cu-Cu (marked by the symbol * in figure 1(a)) are higher than those for $u^2(T, P)$ (Greegor and Lytle 1979).

Figure 3 shows how $C_R(T, P)$ depends on temperature for Cu-Cu, Ag-Ag and Cu_xAg_y under pressure effects. Similar to figures 1 and 2, each correlation function is linearly proportional to T at high temperatures, and the classical limit is applicable. At low temperatures, the curves for Cu-Cu, Ag-Ag and $Cu_{72}Ag_{28}$ contain zero-point energy contributions, which is a quantum effect. The calculated results for $\sigma^2(T, P)$, $u^2(T, P)$, and $C_R(T, P)$ for Cu-Cu, Ag-Ag fit well with the experimental values (Greegor and Lytle 1979, Yokoyama *et al* 1989, Okube and Yoshiasa 2001), and those for $Cu_{72}Ag_{28}$ agree well with other theories (Ba 2020). Thus, it is possible to deduce that the calculation results of the present method for Cu_xAg_{1-x} are reasonable. Moreover, $\sigma^2(T)$ is greater than $u^2(T)$, showing that the damping coefficients in EXAFS of the correlation oscillation model are larger than those of single-particle anharmonic oscillation models.

Figure 4 shows the temperature dependence under pressure effects of the correlation ratio $\sigma^2(T)/C_R(T)u^2(T)$, which decreases rapidly at low temperatures and is unchanged at high temperatures,

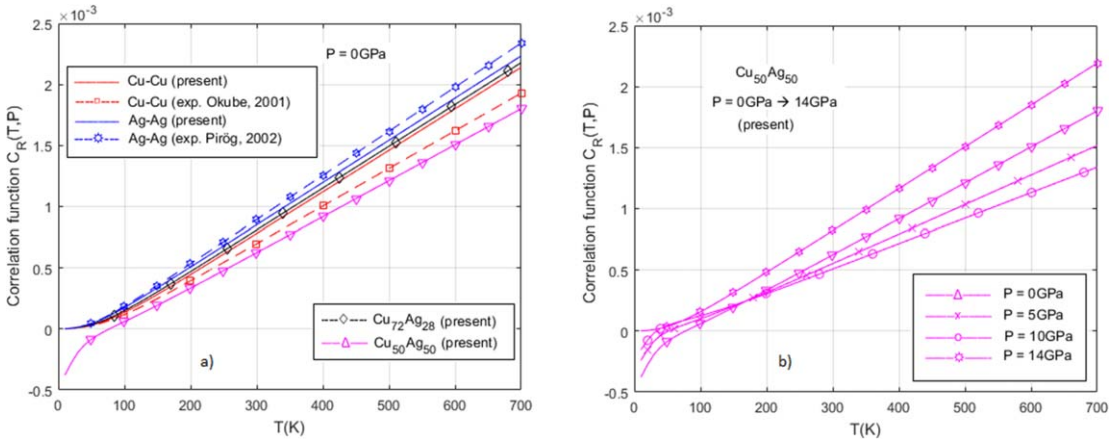

Figure 3. Dependence on temperature and pressure of $C_R(T, P)$ for Cu, Ag, Cu_xAg_{1-x} ($x = 72, 50$) at 0GPa (a); For $Cu_{50}Ag_{50}$ up to 14GPa (b).

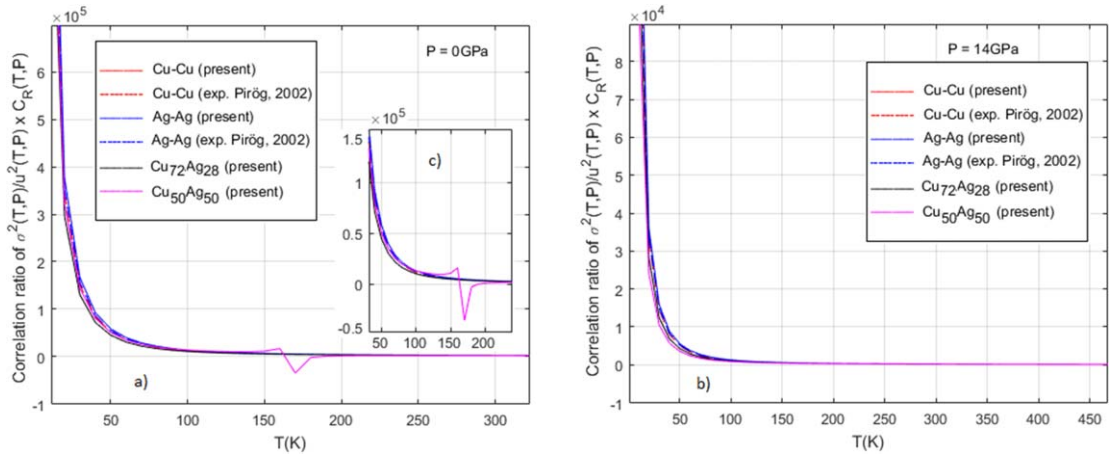

Figure 4. Correlation ratios of σ^2/u^2 C_R at 0GPa (a), and 14GPa (b).

reflecting the correlation effect between these quantities in the classical theories and fitting the curve line inferred from the empirical data (blue and red dashed lines; Pirög *et al* 2002).

Note that the curves in figures 1–4 for the intermetallic alloys $Cu_{72}Ag_{28}$ and $Cu_{50}Ag_{50}$ have attractive characteristics. For $Cu_{72}Ag_{28}$, its curves are similar in shape to those for pure Cu-Cu, Ag-Ag meaning that $Cu_{72}Ag_{28}$ still has an fcc structure. However, for $Cu_{50}Ag_{50}$ (the magenta lines in figures 1(a)–4(a)), the curves are abnormally shaped, contain no zero-point energy, and do not follow those of Cu-Cu, Ag-Ag and $Cu_{72}Ag_{28}$ at low temperatures (in the range of 140–200 K), seen more clearly in figures 4(a), (c). At temperatures higher than 200 K, the curves return gradually to those for Cu-Cu, Ag-Ag and $Cu_{72}Ag_{28}$.

Figures 1(b)–3(b) shows the temperature dependence of the σ^2, u^2, and the C_R, respectively, for $Cu_{50}Ag_{50}$ alloy under pressures effects from 0GPa to 14GPa. As the pressure increases, the curve lines tend to gradually shift according to the curves of Cu-Cu, Ag-Ag crystals and $Cu_{72}Ag_{28}$ alloy. When pressure up to 14GPa, curve lines of $Cu_{50}Ag_{50}$ alloy are similar to those of Cu-Cu, Ag-Ag and $Cu_{72}Ag_{28}$, that mean they are linearly proportional to T at high temperatures and contain zero-point energy contributions at low temperatures, in figure 4 shows that the crease segment in figures 4(a), 4(c) has straightened identical to the other curves at pressure 14GPa (figure 4(b)).

We speculate that for $Cu_{50}Ag_{50}$ with a 1:1 ratio, the atoms are no longer closely linked to each other as in an fcc lattice at low temperatures and pressure, meaning that the alloy $Cu_{50}Ag_{50}$ is impossible in practice in the range temperatures of 140–200 K and pressure is lower than 14GPa due to the atoms' correlation displacement changes suddenly and causes structural disruption. With increasing temperature, the atoms' correlation displacement changes until the temperature reaches a certain value (over 200 K) (or pressure increased up to 14GPa), then the fcc lattice order slowly recovers, and the curves for $Cu_{50}Ag_{50}$ return to those for Cu-Cu, Ag-Ag

and $Cu_{72}Ag_{28}$. This explanation accords entirely reasonably with studies done in other models and theories, and agree well with experimentations for Cu-Ag alloy at 1:1 ratio (Nguyen and Vu 2019, Kraut and Stern 2000).

4. Conclusions

In the present work, the correlation displacement functions, the MSRD, and the MSD in EXAFS spectra and their ratios were deduced and analyzed. The theory was applied to Cu-Cu, Ag-Ag crystals and Cu_xAg_{1-x} alloys, and analytical expressions for $C_R(T, P)$, $\sigma^2(T, P)$, and $u^2(T, P)$ were inferred based on Debye models. The advantage of these models is based on using anharmonic effective potentials, which account for the contributions of all the nearest-neighbor atoms. The differences in the effective SFCs and the numbers and masses of vibrating atoms in these models cause differences in the crystal thermodynamic properties.

At high temperatures and at any pressure, $\sigma^2(T, P)$, $u^2(T, P)$, and $C_R(T, P)$ are all linearly proportional to the temperature T, and the classical limit is applicable. At low temperatures, $\sigma^2(T, P)$, $u^2(T, P)$, and $C_R(T, P)$ of Cu-Cu, Ag-Ag and $Cu_{72}Ag_{28}$ crystals (at any pressure), and for $Cu_{50}Ag_{50}$ alloy (at the pressure 14GPa) contain zero-point energy contributions, which is a quantum effect. The correlation ratio $\sigma^2(T, P)/C_R(T, P)u^2(T, P)$ is constant at high temperatures, reflecting correctly the correlation among these quantities in EXAFS classical theories and agrees well with the curve inferred from empirical data.

The crystal lattice of $Cu_{50}Ag_{50}$ alloy exhibited abnormal disorder at temperatures of the range 140–180 K and the pressure is less than 14GPa. We speculate that this is because the Cu and Ag atoms are no longer linked closely as in an fcc structure, meaning that Cu-Ag alloy with a 1:1 ratio is impossible at temperatures around 140–200 K and the pressure is less than 14GPa. The cause may be that the atoms' correlation displacement changes suddenly and causes structural disruption. This result was discovered by Kraut and Stern (2000) as well as in other theoretical studies by Nguyen and Vu (2019) and Ba (2020). These anomalies may give rise to many new interesting in-depth studies for researchers specializing in materials science.

The good agreement between the calculation results of the present study and the values obtained from experiments and calculations according to other models shows the effectiveness of the present theory for analyzing EXAFS spectral data.

Acknowledgments

One of the authors (Ba Duc Nguyen) thanks Tan Trao University, Tuyen Quang, Viet Nam for the support of this study.

Conflicts of interest

The authors declare that they have no conflicts of interest.

ORCID iDs

Ba Duc Nguyen https://orcid.org/0000-0001-6190-0588

References

Ba D N and Tho V Q 2017 Dependence on the temperature and doped ratio of the cumulants and thermodynamic parameters in XAFS of cubic crystals *Tan Trao University Journal of Science* **3** 34–9

Beni G and Platzman P M 1976 Temperature and polarization dependence of extended x-ray absorption fine-structure spectra *Phys. Rev.* B **14** 1514

Crozier E D, Rehr J J and Ingalls R 1988 *X-ray Absorption: Principles, Applications, Techniques of EXAFS, SEXAFS and XANES* (New York: Wiley) Chap. 9 p 373

Duc N B, Tho V Q, Hiep T P and Quynh L N T 2018 Thermodynamic parameters depend on temperature with the influence of doping ratio of the crystal structure metals in extended x-ray absorption fine structure *Tan Trao University Journal of Science* **4** 5

Frenkel A I and Rehr J J 1993 Thermal expansion and x-ray-absorption fine-structure cumulants *Phys. Rev.* B **48** 585

Greegor R B and Lytle F W 1979 Extended x-ray absorption fine structure determination of thermal disorder in Cu: Comparison of theory and experiment *Phys. Rev.* B **20** 4908

Hung N V and Rehr J J 1997 Anharmonic correlated Einstein-model Debye-Waller factors *Phys. Rev.* B **56** 43

Hung N V, Trung N B, Duc N B, Son D D and Tien T S 2014 Debye-Waller factor and correlation effects in XAFS of cubic crystals *J. Phys. Sci. Applic.* **4** 43

Kraut J C and Stern W B 2000 The density of gold-silver-copper alloys and its calculation from the chemical composition *J. Gold Bull.* **33** 52

Nafi A, Cheikh M and Mercier O 2013 Identification of mechanical properties of CuSil-steel brazed structures joints: a numerical approach *J. Adhes. Sci. Technol.* **27** 2705

Nguyen B D 2020 Application of the Debye model to study anharmonic correlation effects for the CuAgX (X = 72; 50) intermetallic alloy *Phys. Scr.* **95** 105708
Ba D N 2020 Influence of temperature and pressure on cumulants and thermodynamic parameters of intermetallic alloy based on anharmonic correlated Einstein model in EXAFS *Phys. Scr.* **5** 31
Nguyen B D, Tho V T, Hiep T P, Nghia N V, Minh P T H and Thanh V T H 2020 Investigation of the anharmonic correlation effects by Debye model in X-ray absorption fine structure spectra - Application to a two component alloy *Dalat Univ. Sci.* **10** 77
Nguyen B D and Vu Q T 2019 Dependence of cumulants and thermodynamic parameters on temperature and doping ratio in extended x-ray absorption fine structure spectra of cubic crystals *Physica B Condens. Mat.* **55** 1
Okube M and Yoshiasa A 2001 Anharmonic effective pair potentials of group VIII and Lb Fcc metals *J. Synchrotron Radiat.* **8** 937
Pirög I V, Nedoseikina T I, Zarubin A I and Shuvaev A T 2002 Anharmonic pair potential study in face-centred-cubic structure metals *J. Phys. Condens. Matter* **14** 1825
Schowalter M, Rosenauer A, Titantah J T and Lamoen D 2009 Computation and parametrization of the temperature dependence of Debye–Waller factors for group IV, III–V and II–VI semiconductors *Acta Cryst.* A **65** 5
Stern E A, Livins P and Zhang Z 1991 Thermal vibration and melting from a local perspective *Phys. Rev.* B **43** 8850
Tranquada J M and Ingalls R 1983 Extended x-ray absorption fine-structure study of anharmonicity in CuBr *Phys. Rev.* B **28** 3520
Yokoyama T, Sasukawa T and Ohta T 1989 Anharmonic interatomic potentials of metals and metal bromides determined by EXAFS *Jpn. J. Appl. Phys.* **28** 1905